Graded bidirectional synaptic plasticity is composed of switch-like unitary events

Daniel H. O'Connor, Gayle M. Wittenberg, and Samuel S.-H. Wang*

Department of Molecular Biology and Program in Neuroscience, Princeton University, Princeton, NJ 08544

Biological information storage events are often rapid transitions between discrete states. In neural systems, the initiation of bidirectional plasticity by all-or-none events may help confer robustness on memory storage. Here, we report that at CA3–CA1 hippocampal synapses, individual potentiation and depression plasticity events are discrete and heterogeneous in nature. Individual synapses began from extreme high and low strength states. Unitary plasticity events were all-or-none and drove synaptic strength between extremes in <1 min. Under naïve conditions, approximately three-fourths of synapses began in a low-strength state. The timing of these unitary events can account for the time course of macroscopic synaptic plasticity.

Both increases (long-term potentiation, LTP) (1) and decreases (long-term depression, LTD) in synaptic strength are almost always measured macroscopically across populations of synaptic contacts (2). Macroscopic recordings, in which plasticity appears as a graded phenomenon, have ranged from extracellular recordings from many thousands of synapses (3, 4) to single-cell recordings (5), including recordings from connected pairs of nearby single neurons representing summed activity from order 10 synaptic terminals (6, 7).

Plasticity has been described in terms of transitions among distinct states (7). However, the concept of synaptic states has not been explored in terms of unitary synaptic strength. Characterizing plasticity at this level requires observations from putative single terminals.

An attractive system for studying unitary plasticity events is the hippocampal CA3–CA1 pathway (4, 8), where connected CA3 and CA1 neurons communicate typically by a single synaptic contact (9). Minimal stimulation techniques (10–12) allow plasticity transitions to be localized in time as they occur (13). Previous work (13) indicates that unitary synaptic potentiation, at least in its initial stages, may be an all-or-none event.

Here, we report on the unitary properties of the initiation of potentiation and depression at CA3–CA1 synapses. We find that both potentiation and depression events are all-or-none and sudden. These events can be reconstituted to account for the time course of plasticity on a macroscopic scale.

Methods

Slice Preparation. Transverse hippocampal slices (300 μm) from Sprague–Dawley rats (postnatal day 13–21) were cut in ice-cold artificial cerebrospinal fluid (ACSF) comprising (in mM) 126 NaCl, 3 KCl, 1 NaH$_2$PO$_4$, 25 D-glucose, 25 NaHCO$_3$, 2 CaCl$_2$, and 1 MgCl$_2$ saturated with 95% O$_2$/5% CO$_2$, incubated at 34°C for 10–15 min, and transferred to a room-temperature interface chamber for ≥60 min before recording. The cutting angle was such that excitatory postsynaptic current (EPSC) size in response to stimulation of stratum radiatum decreased rapidly as the stimulation electrode was moved toward CA3. By using this cutting angle and moving the stimulation electrode as far toward CA3 as possible, we reduced the likelihood of stimulating multiple connected axons. For recordings, slices were transferred to an immersion-type chamber and perfused at 2–4 ml/min with ACSF at 23–26°C, except for three perforated-patch experiments at 35°C.

Electrophysiology. CA1 pyramidal neurons were recorded by blind conventional whole-cell or perforated-patch methods and voltage-clamped to −70 mV. Patch pipettes (2–5 MΩ) were filled with (in mM) 133 methanesulfonic acid, 7.4 CsCl, 0.3 MgCl$_2$, 10 NaHepes, 0.2 EGTA, 3 Na$_2$ATP, and 0.3 Na$_2$GTP (pH 7.3 with CsOH, 290 milliosmolar). Whole-cell experiments were terminated after 13 min, 5 min after the end of the plasticity induction protocol. For perforated recordings, pipettes were tip-filled with pipette solution and backfilled with solution containing up to 0.48 mg/ml amphotericin B and up to 0.16 mg/ml gramicidin D (Sigma). Experiments began when series resistance had stabilized (32 ± 14 MΩ, mean ± SD, compared with 25 ± 12 MΩ for conventional whole-cell recordings), usually within 25–45 min. Series resistance was monitored for abrupt changes indicating rupture of the membrane. Liquid junction potentials were not corrected. We used younger animals (mostly postnatal day 13–16) to increase the probability of isolating single inputs (13, 14).

Population EPSCs were elicited with a concentric bipolar steel electrode (50-μm diameter inner pole and 200-μm diameter outer pole, FHC, Bowdoinham, Maine) placed in stratum radiatum >200 μm from the recording pipette. For minimal stimulation, the electrode was an ACSF-filled patch pipette. Often, this stimulation pipette had to be moved to several locations before minimal stimulation could be achieved. At each final location, a stimulus–response curve was obtained by varying the stimulus current and recording the resulting EPSC amplitudes (e.g., black circles in Fig. 2a). In whole-cell experiments, this curve was sampled less finely than in perforated-patch experiments to avoid washout of LTP. Stimuli were given at 10–130 (mean 60) μA for a duration of 0.1 ms. Putative single-synapse responses were identified by using the following criteria (11, 12, 15): (i) the mean amplitude and failure rate of responses were insensitive to changes of stimulus intensity of at least 10%, (ii) decreasing the stimulus strength led to an abrupt and total failure of the response, and (iii) response latency did not change over the course of the experiment. Stimulation occurred at 1 Hz throughout the recordings, a frequency that does not evoke short-term presynaptic enhancements in transmitter release and is not expected to lead to depression under postsynaptic voltage clamp (16). Picrotoxin (100 μM) or bicuculline (10 μM, Sigma) was included in the ACSF. For perforated-patch recordings, the ACSF included 0.5–1 mM glutamine (Sigma) to reduce the depletion of glutamate in presynaptic terminals (17). Responses were measured after subtracting either failures or responses measured in 10 μM 6,7-dinitroquinoxaline-2,3-dione (DNQX) (Sigma) at the end of the experiment. The average probability of release was estimated as 1 minus twice the proportion of EPSCs with negative amplitude (18). The average release probability thus estimated was 0.54 for experiments with DNQX subtraction.
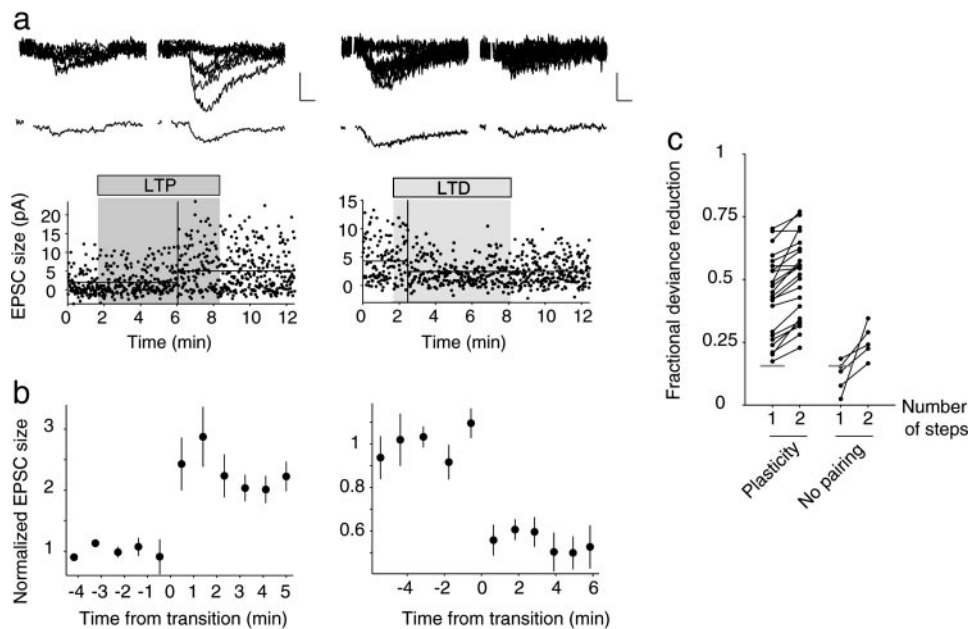
LTP induction consisted of continued presynaptic stimulation and pairing every 10th stimulus with a depolarization to 0 mV 40

NEUROSCIENCE

Fig. 1. Unitary plasticity events take place in single steps. (*a*) At single synapses, potentiation (*Left*) and depression (*Right*) events are step-like. (*Upper*) Ten consecutive sweeps from before (*Left*) and after (*Right*) plasticity; the means are shown below. (Scale bars, 10 pA and 5 ms.) (*Lower*) EPSC time series. Vertical lines show transition times. (*b*) Grouped and aligned averages of plasticity events. (*c*) Deviance reduction analysis. (*Left*) The amount of deviance reduction from splitting data sets in which plasticity events occurred. Reductions are shown for introducing one or two breaks. (*Right*) The same analysis for data in which no plasticity protocol was given. Gray lines indicate the maximum deviance reduction seen in 90% of data sets with no plasticity, generated by shuffling control data sets (see *Methods*). Deviance reduction was done on data binned 10 responses per point.

times. LTD induction consisted of pairing every third stimulus with a depolarization to −55 mV 130 times. Depolarizations lasted 700 ms and began 150 ms before the stimulus.

Data were acquired with an Axopatch-1D amplifier, filtered at 1–2 kHz, and analyzed with custom MATLAB software. Response amplitudes were measured in a 2-ms window at the peak of the EPSC. Experiments were rejected if series resistance changed >30%. In minimal stimulation experiments, outlier observations >3 SD from mean were trimmed. Error bars are SEM unless otherwise indicated.

Analysis of Minimal Stimulation Experiments. To determine whether plasticity occurred, a breakpoint in the EPSC time series was found that minimized the sum of squares deviance D, computed as

$$D(t) = \sum_{i=1}^{t} \left(x_i - \frac{1}{t} \sum_{j=1}^{t} x_j \right)^2 + \sum_{i=t+1}^{n} \left(x_i - \frac{1}{n-t} \sum_{j=t+1}^{n} x_j \right)^2, \quad [1]$$

where $t = 1, 2, \ldots n$ is the time of each possible breakpoint. Each summation is a measure of the variation of a data set around its mean. Breaking a data set reduces total deviance by restricting comparisons to the mean calculated on the same side of the breakpoint. Breaking the data at a true transition time should therefore maximally reduce total deviance. To fit two breakpoints (Fig. 1c), the locations of both were varied simultaneously.

To put a confidence interval on the deviance reduction that would be obtained in the absence of plasticity. EPSC time series from five control experiments in which no plasticity protocols were given were shuffled randomly to yield 5,000 simulated data sets.

To characterize the time course of transitions, data were averaged by using 10-response bins and fitted by least squares to ramp functions. We used ramp functions rather than sigmoid curves because the ramp functions allowed us to search exhaustively for the global best fit without the problem of convergence to local minima.

Maximum Likelihood Analysis. To answer the question of what true transition time was most consistent with our data, we compared the fitted ramp durations from real data to ramp durations calculated from simulated data with artificially added known ramp transitions. For each transition time, 460 simulated data sets were generated with the time of plasticity onset selected randomly (Fig. 3d).

Alignment of these data sets by the same procedure used for real data generates a small apparent step at the found breakpoint ($t = 0$), but the overall time course is still clearly a ramp (Fig. 3c *Center*).

The distribution of best fitted ramp times corresponding to an artificially generated true transition time T was estimated by filtering the histogram of fitted ramp durations with a Gaussian kernel (width $\sigma = 15$ s) and normalizing. The likelihood that the fitted ramp durations t_i from real data were drawn from that distribution was calculated as

$$L(T) = \prod_i p(t_i, T),$$

where $p(t_i, T)$ is the distribution of fitted ramp times t_i for a given T. The true transition time was then taken to be the value that maximized $L(T)$.

Confidence intervals on T were determined by a bootstrapping method in which N observations were repeatedly drawn at random (with replacement) from the real data set of N observations. The maximum likelihood procedure was carried out on these resampled data to obtain a histogram of most-likely fitted ramp times, $H(t)$. The 90% confidence interval always included 0 s (a step) and was bounded above by the time t_{90} at which $\Sigma(H \le t_{90}) = 0.9\Sigma H$. One outlier depression data point was excluded from the maximum likelihood analysis because the procedure was sensitive to this outlier when applied to subsets of the data.

Results

To investigate unitary synaptic plasticity events, we performed 37 minimal stimulation experiments in acute hippocampal slices: 18 perforated-patch recordings and 19 conventional whole-cell recordings. To investigate bidirectional plasticity in synaptic populations, we performed 12 whole-cell experiments under nonminimal conditions.

Under conditions of minimal synaptic stimulation (Fig. 1a), a presynaptic action potential results in a mixture of neurotransmitter release successes and failures (10–12). We measured synaptic strength as an average of all responses. To eliminate stimulus frequency-dependent effects such as facilitation and short-term depression (19), we gave stimuli at a constant rate (1 Hz) throughout all recordings while keeping the postsynaptic cell in voltage clamp. To evoke potentiation and depression, we paired stimuli

Fig. 2. Isolation and stability of minimal responses. (*a*) Recruitment of a presumed single afferent axon with increasing stimulus intensity. (*Left*) As the stimulus current is increased, there is a period of presumed intermittent axon recruitment at the threshold, and then a plateau of response. The stimulus–response relationship is little changed after 25 and 60 min. (*Right*) Mean responses at subthreshold and suprathreshold stimulation currents (average of 10 sweeps each). (Scale bars, 10 pA and 20 ms.) (*b*) The stimulation electrode was moved along its axis. Responses were limited to a region of a few microns. Stimulation current was 16 μA. (*c*) Cumulative histograms of first (solid) and second (dashed) EPSC amplitudes in response to paired stimulus pulses (40-ms interval; $n =$ 164). The second EPSC [release probability (Pr) = 0.50 ± 0.04] shows kinetics similar to the first (Pr = 0.58 ± 0.04). (*Inset*) Average of all responses. (Scale bars, 10 pA and 20 ms.) (*d*) Baseline EPSCs in response to stimulation at 1 Hz. Cumulative histograms (200 responses each) show a stable amplitude distribution. All data come from two minimal stimulation sites.

with depolarization. When given as the first conditioning protocol ("naïve synapses"), pairing of synaptic activation with postsynaptic depolarizations to 0 mV (Fig. 1*a Left*; ref. 13) led to increases in synaptic strength in three of eight whole-cell recordings and six of nine perforated recordings and no change in the other eight recordings. Conversely, pairing with depolarization to −55 mV (Fig. 1*a Right*) led to decreases in synaptic strength in 4 of 8 whole-cell recordings and 1 of 7 perforated recordings and no change in the other 10 recordings. Pairing protocols given later during each experiment could also lead to plasticity. When these additional events were included, a total of 21 potentiation events and 12 depression events were observed. These changes persisted until subsequent protocols induced plasticity or for the remaining duration of the recordings (from 1 to 21 min after the plasticity event; mean = 10 min, $n = 33$). Thus, our experimental conditions can capture the initiation of bidirectional synaptic plasticity.

We quantified the step-like nature of these plasticity events in three ways. (*i*) We identified the location of the optimal split in the data by maximum deviance reduction (examples, Fig. 1*a*; aligned averages, Fig. 1*b*). (*ii*) In experiments showing plasticity, we calculated the additional reduction in deviance that results from searching for two breakpoints rather than one (Fig. 1*c*). (*iii*) We estimated the duration of the transition time of plasticity events by maximum likelihood analysis comparisons with simulated data (Fig. 3).

The size of potentiation and depression events could be measured by fitting data to step functions (Fig. 1*a*). For naïve synapses undergoing first-time plasticity, this reduced the deviance, a measure of the remaining variability after fitting to a step [Fig. 1*c*; deviance reduction = $44 \pm 16\%$ (mean $\pm$ SD); $n = 23$]. In all pooled plasticity events, potentiating synapses showed increases to $123 \pm 13\%$ (mean $\pm$ SEM) above the preconditioning baseline, and depressing synapses showed decreases to $52 \pm 3\%$ below baseline.

This deviance reduction was significantly greater than that observed by fitting steps to experiments in which no pairings were given [Fig. 1*c*; deviance reduction = $11 \pm 6\%$ (mean $\pm$ SD); $n = 5$; significantly different from plasticity experiments, $P < 0.0001$, one-tailed Student's *t* test] or simulated data sets ($8 \pm 4\%$ deviance reduction; $n = 5,000$; $P < 0.0001$, one-tailed *t* test). No plasticity experiment showed an amount of deviance reduction smaller than that seen in 90% of the simulated data sets (gray lines in Fig. 1*c*) compared with four of the five no-pairing experiments (Fig. 1*c*).

Thus, the steps identified by our deviance reduction analysis are likely to reflect true plasticity events rather than spurious steps.

To test whether a single step was an adequate description of the data, we examined the amount of deviance reduction achieved by dividing the data at one or two breakpoints. Assigning two breakpoints gave slightly better fits (deviance reduction = $51 \pm 16\%$; Fig. 1*c*) than at one breakpoint. The increase in deviance reduction over single-step fits was $7 \pm 5\%$, not greater than the increment obtained in control data (difference in control data between two breakpoints and one breakpoint = $14 \pm 11\%$; one-tailed *t* test, $P = 0.98$). We conclude that a single-step function is sufficient to describe these plasticity events. This conclusion is consistent with the idea that synapses underwent at most one major plasticity step.

These step-like plasticity data are consistent with reliable activation of a single synapse. Four observations made in experiments selected by the same criteria used to accept our plasticity experiments (Fig. 2) suggest that our activation was single-axon and stable. First, stimulus intensity–EPSC curves show a steep onset and a plateau of unchanging response recruitment (11) (Fig. 2*a*). Second, by moving the stimulation electrode along its axis, we observed a region of stable postsynaptic response extending a few microns (Fig. 2*b*). Third, analysis of paired pulses shows that the kinetics and amplitude distributions of the first and second responses are similar (14, 15). Fourth, baseline EPSCs taken at 1 Hz are stable and do not show systematic plasticity. Finally, even if in some experiments we were activating multiple synapses (either nonplastic synapses or synapses that undergo plasticity in tandem), in these scenarios single-synapse depression and potentiation would still be all-or-none events.

Although unitary plasticity events required many pairings, when they did occur, they appeared to be quite abrupt (Fig. 3 *a* and *b*). To quantify the sharpness of these transitions, for each first-time plasticity event, we fitted the binned data using ramp functions (Fig. 3 *a Bottom* and *b Bottom*). The best-fitted ramp times were predominantly shorter than 100 s (red curve in Fig. 3*d*). The median best-fit ramp time was 14 s (range = 12–534 s; $n = 15$) for potentiation events and 17 s (range = 16–346 s; $n = 8$) for depression events, near the minimum limit set by the 10-s bin size.

Because of fluctuations in measured synaptic responses over time, the particular noise present might have distorted the apparent time course of plasticity, making transitions appear more steep or shallow than they really are. As a more rigorous test, we generated

Fig. 3. Step-like time course of plasticity events. (*a*) Example of a potentiation event from a perforated-patch recording. (*Top*) Ten consecutive sweeps before (*Left*) and after (*Right*) potentiation. The means are shown below. (Scale bars, 10 pA and 5 ms.) (*Middle*) EPSC time series from the same experiment. Vertical line indicates transition time. (*Bottom*) Same data binned (10 responses per point) and fitted to the best ramp function (ramp duration = 12 s). (*b*) Example of a depression event from a perforated-patch experiment (ramp duration = 107 s). Same conventions as in *a*. (*c*) Application of analysis methods to simulated data sets. (*Left*) Three control experiments with no plasticity protocol, binned 10 responses per point, aligned using the procedure in Fig. 1*c*, and averaged. The same procedure applied to simulated data generated by multiplying control data with either a ramp spanning the length of the standard pairing period (*Center*) or by a step function (*Right*). (*d*) The red trace shows the cumulative histogram of best-fit ramp times for all plasticity events. The black curves show the corresponding cumulative histograms for simulated step transitions and for ramps of duration 50–300 s.

simulated data sets with known transition times (Fig. 3*c*) and used fits to these data sets as a standard of comparison to identify the most likely transition time underlying the distribution of fitted times from real data (Fig. 3*d*). Artificial data sets were constructed by multiplying control data (from no-pairing control experiments or from experimental data before the first plasticity event) by either a ramp or step function corresponding to 2-fold depression or potentiation. The ratio of upward to downward events was the same as in the real data set. Fits to simulated data (black curves in Fig. 3*d*) gave apparent ramp times that varied widely, with a large number of apparent step-like transitions.

Based on comparisons to these fits, the most likely ramp time in the real data (depression and potentiation events pooled) was 0 s, a step transition (90% confidence interval, 0–51 s). In subsets of the data, the resolving power was somewhat lower. For potentiation events alone, the most likely transition time was 0 s (90% confidence interval, 0–30 s), and for depression events, it was 30 s (90% confidence interval, 0–116 s). We conclude that potentiation and depression events occur on the time scale of 1 min or less, and, under our stimulation conditions, these events cannot be distinguished from step transitions.

The occurrence of plasticity in single steps raises the possibility that individual synapses might move between extreme high and low levels of strength. An intermediate-strength level is possible if depression and potentiation can both occur starting from the same initial level of strength (20). To test for this possibility, we induced potentiation and depression events in the same recording (Fig. 4). Perforated-patch recordings (12) allowed us to make extended recordings without washing out LTP induction mechanisms (21).

When given first, a depression protocol was rarely successful in inducing depression (Fig. 4*a*; one of seven cells), suggesting that

synapses typically start from relative low strength. In contrast, after potentiation was induced, LTD protocols were successful in inducing depression in 7 of 10 cells (different from the naïve case; Pearson's χ^2 = 5.13, 1 df; $P < 0.05$). The other three cells that did not depotentiate may reflect the resistance to depotentiation previously observed across populations of synapses (7). Conversely, when an LTP protocol was given first, potentiation occurred in six of nine cells. However, after an LTD protocol, subsequent LTP protocols induced potentiation in all 12 of 12 cells (different from the naïve case; Pearson's χ^2 = 4.67, 1 df; $P < 0.05$). Overall, naïve synapses that could not potentiate could later depress ($n = 3$), and naïve synapses that could not depress could later potentiate ($n = 6$). Taken together, these experiments suggest that synapses start from extreme high and low levels of strength.

If synapses begin in an intermediate level of strength, second jumps in strength would tend to be larger in amplitude than first jumps, giving overshoots or undershoots. To test for this, we examined experiments in which plasticity could be reversed (Fig. 4*b*). In Fig. 4*b*, overshoot of potentiation over depression is visible as upright triangle symbols above the diagonal; undershoot is visible as inverted triangle symbols below the diagonal. Only three of eight reversal experiments showed overshoot/undershoot, indistinguishable from the chance expectation of four of eight. Thus, under our conditions, synapses generally do not appear to start from an intermediate level of strength. Overall, depression and potentiation events were comparable in size to one another (ratio of potentiation step size to depression step size = 1.2 ± 0.2; $n = 8$; not significantly different from 1 by two-tailed t test, $P = 0.4$; Fig. 4*b*). In individual experiments, event sizes were not exactly matched (Fig. 4*b*), indicating that while plasticity drives synaptic strength between saturated extremes, the levels of those extremes can vary.
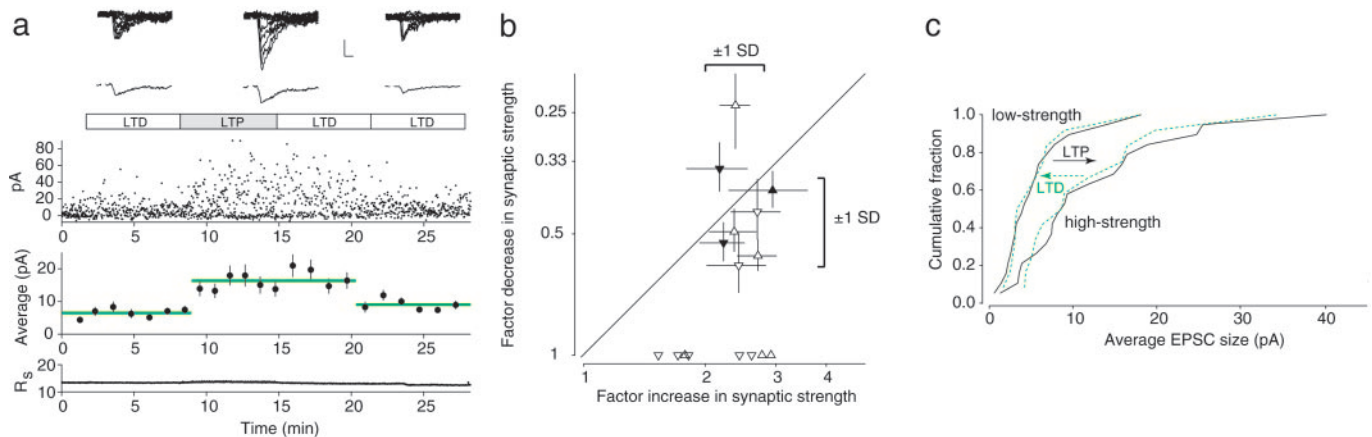
Fig. 4. Multiple plasticity events in single synapses. (*a*) Single-synapse responses from a perforated-patch recording. (*Top*) Ten consecutive sweeps before and after potentiation and after depression. The averages are shown below. (Scale bars, 20 pA and 5 ms.) (*Middle*) EPSC time series from the same experiment. Each labeled bar indicates an LTD or LTP induction protocol. (*Bottom*) A 50-response binned average shows that initial LTD pairing did not induce depression. After potentiation, subsequent LTD pairing returned synaptic strength to a low value. Series resistance is shown below. (*b*) Changes in strength in response to multiple induction protocols with LTP pairing given first (△) or LTD pairing given first (▽). Filled symbols indicate recordings at 35°C. Error bars are SEM. The brackets indicate ±1 SD ranges from pooled whole-cell and perforated-patch experiments. For this graph, only the first two plasticity events per recording were used. (*c*) Cumulative histograms of low and high levels of strengths for all potentiation (black lines) and all depression (green lines) events.

If synapses move between extreme high and low levels of strength, the distributions of high and low strengths should be similar in potentiation and depression events. We plotted the cumulative distributions of response amplitudes before and after inducing potentiation or depression (Fig. 4*c*). The distributions of "high" strengths (predepression responses and postpotentiation responses) were similar to one another (right-hand histograms in Fig. 4*c*; not different by two-sample Kolmogorov–Smirnov test, $P = 0.9$). Likewise, the distributions of "low" strengths (postdepression responses and prepotentiation responses) were also similar (left-hand histograms in Fig. 4*c*; not different by two-sample Kolmogorov–Smirnov test, $P > 0.99$). On average, potentiation events (a low-to-high jump of 6.1 ± 1.4 pA from 5.9 ± 1.1 to 12.1 ± 2.0 pA; mean $\pm$ SEM; $n = 21$) and depression events (a high-to-low drop of 6.2 ± 1.4 pA from 11.8 ± 2.6 to 5.5 ± 1.3 pA; $n = 12$) were not of different size ($P = 0.9$, two-tailed t test). Overall, these experiments are consistent with two extremes of strength per synapse.

A two-level model suggested that we could estimate the relative occupancy of the two levels. In each recording, we assigned a value of low strength if the naïve synapse could potentiate or was unable to depress and assigned a value of high strength if the naïve synapse could depress or was unable to potentiate. This analysis was restricted to perforated recordings because LTP induction mechanisms are washed out by whole-cell recording (21). In synapses that received multiple conditioning protocols, these initial assignments were consistent with later plasticity events, except for the three recordings in which potentiation could not be reversed by later depression protocols. All synapses eventually depressed or potentiated. Under these definitions, 12 of 17 (0.71 ± 0.11) synapses started at a low level, and 0.29 ± 0.11 of synapses started at a high level (mean $\pm$ SD calculated assuming binomial statistics).

Another measure of level occupancy extending over a longer time than single-cell experiments can be obtained from extracellular field potential recording. This estimate can be made by comparing baseline strength with saturated LTD and LTP (22). LTP saturated by theta-burst stimulation gave a $129 \pm 11\%$ increase from baseline, and LTD saturated by using prolonged stimulation at 1 Hz gave a decrease of $35 \pm 3\%$ below baseline (Fig. 5*a*). Assuming that the size distribution of low-to-high jumps was the same as that of high-to-low drops, the starting proportion of plastic synapses with low strength was $129/(129 + 35)$ or 0.79 ± 0.02, and 0.21 ± 0.02 had high strength. Therefore, based on both

perforated recordings and field recordings, in this preparation, approximately three-fourths of synapses start from low strength.

To test whether unitary plasticity events were sufficient to account for the short-term properties of synaptic plasticity, we compared the temporal distribution of unitary events to the time
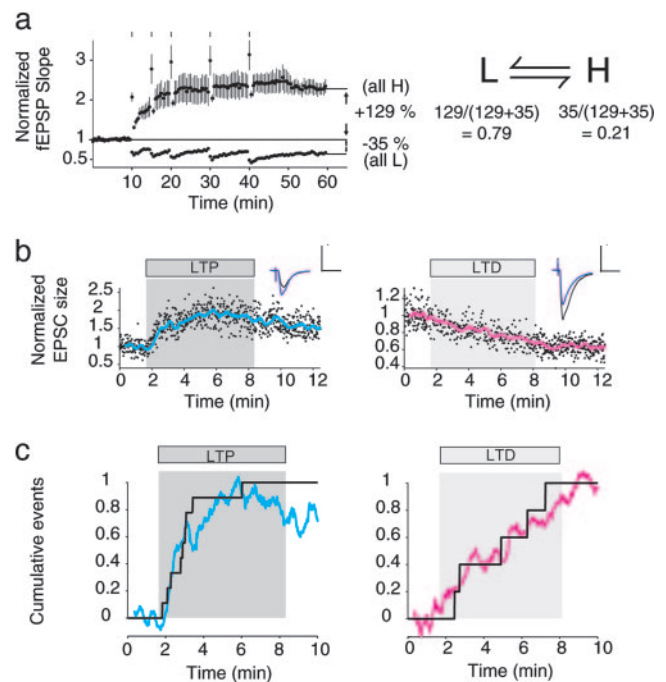
Fig. 5. Macroscopic plasticity in terms of unitary events. (*a*) Extracellular field recording. Saturated population LTP (*Upper*) exceeded saturated population LTD (*Lower*), indicating that most synapses begin from low strength. Green marks show times of theta-burst stimuli (*Upper*) (first mark, four episodes; each subsequent mark, one episode) or low-frequency stimuli (*Lower*) (500 at 1 Hz). (*b*) In synaptic populations, potentiation (*Left*) ($n = 7$) and depression (*Right*) ($n = 5$) appear graded. Shaded regions indicate pairings. Data are pointwise averages, and the trace shows a 20-point moving average. Sample sweeps are averages of 100 responses. (Scale bars, 50 pA and 20 ms.) (*c*) Cumulative histograms of transition times (whole-cell and perforated-patch data were pooled) with population time courses from *a* superimposed.

NEUROSCIENCE

course of LTP and LTD measured under nonminimal conditions. In whole-cell experiments in which populations of synapses were activated, potentiation and depression protocols resulted in plasticity with graded time courses that, by the end of the pairing protocol, reached $75 \pm 19\%$ above baseline ($n = 7$) and $34 \pm 7\%$ below baseline ($n = 5$), respectively (Fig. 5b).

Next, in minimal-stimulation whole-cell recordings, we extracted the distribution over time of potentiation and depression events. Because pairing protocols may induce changes in NMDA receptors and therefore the precise activity dependence of potentiation (23), only data from naïve synapses were used. These transition times occurred early in LTP experiments and later in LTD experiments: Potentiation occurred after 8 ± 7 pairings (mean $\pm$ SD; range = 1–26 pairings; $n = 9$), and depression occurred after 61 ± 42 pairings (range = 16–112 pairings; $n = 5$). For both potentiation and depression, the cumulative histograms of event times closely followed the scaled time courses of LTP and LTD from whole-cell nonminimal stimulation experiments (Fig. 5c). Thus, the distribution of unitary plasticity events can account for the time course of LTP and LTD in synaptic populations.

Discussion

We find that at single CA3–CA1 synapses, the induction of plasticity drives synapses to extremes of strength in upward and downward steps. These steps are all-or-none, saturating synapses to full potentiation or depression for many minutes after induction. These unitary steps can account for the time course of macroscopic LTP and LTD. Overall, our observations indicate how heterogeneous unitary events distributed over time add up to form the macroscopic phenomenon of bidirectional plasticity.

Our measurements extend and complement previous work on synaptic state transitions during potentiation (13). We find that depression events are also sudden, taking place on the time scale of seconds. Both potentiation and depression saturate synaptic strength, making bidirectional plasticity a transition between extremes. Potentiation and depression events are, on average, ≈2-fold changes in strength. The distributions of synaptic strengths before and after inducing plasticity are, within measurement error, matched (Fig. 4c). Taken together, this evidence indicates that at the unitary level, synaptic plasticity has several characteristics of an all-or-none switch.

Although it may seem surprising that plasticity would be initiated by all-or-none decisions, this result can be reconciled straightforwardly with known mechanisms of induction. A key step in inducing LTP at the CA3–CA1 synapse is the activation of calmodulin-dependent kinase II, which can phosphorylate itself to a form that no longer requires calcium. Thus, a large triggering calcium signal (24) is thought to be able to drive kinases all of the way to full activation (25). Detailed mechanistic modeling of the kinase–phosphatase system (25) suggests that the converse downward step, which requires phosphatases and is triggered by a prolonged, smaller calcium signal (24), would also be an all-or-none step.

If induction is a binary event, then the initial expression of plasticity would be expected to be all-or-none, which is true even though LTP and LTD may be initially expressed presynaptically (26), postsynaptically (20, 26–28), and even morphologically (29). LTP and LTD can reverse one another (2, 30), indicating common final target(s) of expression, and a shared triggering event with all-or-none properties would be likely to drive multiple expression mechanisms in tandem. Indeed, our transition time analysis suggests that mechanisms of plasticity are approximately synchronized and that a synapse is ultimately pushed over the threshold for plasticity by as little as one pairing event. On a longer time scale, step-like changes of synaptic strength give way to longer-term events that may take a more continuous character.

On the time scale of our plasticity experiments, synapses can be described as occupying states of low and high strength. In this schematic model, synapses in acutely prepared brain slices begin in a mixture of states. This model is consistent with previous data from connected neuronal pairs in slice culture (31), suggesting that the terminals joining two neurons start from heterogeneous levels of strength and can often be all maximally potentiated or depressed. The strength of the low and high states may vary across the population and over time. Our suggested low state may also include "silent" synapses in which no α-amino-3-hydroxy-5-methyl-4-isoxazolepropionic acid (AMPA) receptor-based synaptic currents are detectable (32). Exploring this possibility in the future will require recording conditions and animal ages that permit identification of silent synapses or the induction of silencing (33).

Binary decisions have many precedents in biology. Examples include lytic/lysogenic growth phases in viruses (34), running/tumbling in flagellar bacteria (35), oocyte maturation (36), and the action potential (37). In these phenomena, the lack of synchronization in populations makes it necessary to perform unitary measurements to reveal the binary nature of the underlying events (38).

As a means of storing information, graded change (39, 40) is more susceptible to drift than all-or-none plasticity (13). Thus, storage of new information in synaptic networks may have a quality that helps make artificial memory storage systems robust: discreteness (41). Our observation of bidirectional all-or-none transitions in strength is reminiscent of transitions between low and high voltage in electronic devices and can be interpreted as a change in one bit of information per plasticity decision.

1. Sanes, J. R. & Lichtman, J. W. (1999) *Nat. Neurosci.* **2,** 597–604.
2. Dudek, S. M. & Bear, M. F. (1992) *Proc. Natl. Acad. Sci. USA* **89,** 4363–4367.
3. Bliss, T. V. P. & Lømo, T. (1973) *J. Physiol.* **232,** 331–356.
4. Bliss, T. V. P. & Collingridge, G. L. (1993) *Nature* **361,** 31–39.
5. Barrionuevo, G. & Brown, T. H. (1983) *Proc. Natl. Acad. Sci. USA* **80,** 7347–7351.
6. Markram, H., Lübke, J., Frotscher, M. & Sakmann, B. (1997) *Science* **275,** 213–215.
7. Montgomery, J. M. & Madison, D. V. (2002) *Neuron* **33,** 765–777.
8. Malenka, R. C. & Nicoll, R. A. (1999) *Science* **285,** 1870–1874.
9. Sorra, K. E. & Harris, K. M. (1993) *J. Neurosci.* **13,** 3736–3748.
10. Bekkers, J. M. & Stevens, C. F. (1990) *Nature* **346,** 724–729.
11. Raastad, M. (1995) *Eur. J. Neurosci.* **7,** 1882–1888.
12. Isaac, J. T., Hjelmstad, G. O., Nicoll, R. A. & Malenka, R. C. (1996) *Proc. Natl. Acad. Sci. USA* **93,** 8710–8715.
13. Petersen, C. C., Malenka, R. C., Nicoll, R. A. & Hopfield, J. J. (1998) *Proc. Natl. Acad. Sci. USA* **95,** 4732–4737.
14. Hsia, A. Y., Malenka, R. C. & Nicoll, R. A. (1998) *J. Neurophysiol.* **79,** 2013–2024.
15. Dobrunz, L. E. & Stevens, C. F. (1997) *Neuron* **18,** 995–1008.
16. Christie, B. R., Magee, J. C. & Johnston, D. (1996) *Learn. Mem.* **3,** 160–169.
17. Larkman, A. U., Jack, J. J. & Stratford, K. J. (1997) *J. Physiol.* **505,** Part 2, 457–471.
18. Liao, D., Hessler, N. A. & Malinow, R. (1995) *Nature* **375,** 400–404.
19. Zucker, R. S. & Regehr, W. G. (2002) *Annu. Rev. Physiol.* **64,** 355–405.
20. Lee, H.-K., Barbarosie, M., Kameyama, K., Bear, M. F. & Huganir, R. L. (2000) *Nature* **405,** 955–959.
21. Malinow, R. & Tsien, R. W. (1990) *Nature* **346,** 177–180.
22. O'Connor, D. H., Wittenberg, G. M. & Wang, S. S.-H. (2005) *J. Neurophysiol.*, in press.
23. Xiao, M.-Y., Wigström, H. & Gustafsson, B. (1994) *Eur. J. Neurosci.* **6,** 1055–1057.
24. Yang, S.-N., Tang, Y.-G. & Zucker, R. S. (1999) *J. Neurophysiol.* **81,** 781–787.
25. Lisman, J. E. & Zhabotinsky, A. M. (2001) *Neuron* **31,** 191–201.
26. Palmer, M. J., Isaac, J. T. & Collingridge, G. L. (2004) *J. Neurosci.* **24,** 4903–4911.
27. Shi, S.-H., Hayashi, Y., Petralia, R. S., Zaman, S. H., Wenthold, R. J., Svoboda, K. & Malinow, R. (1999) *Science* **284,** 1811–1816.
28. Ehlers, M. D. (2000) *Neuron* **28,** 511–525.
29. Matsuzaki, M., Honkura, N., Ellis-Davies, G. C. R. & Kasai, H. (2004) *Nature* **429,** 761–766.
30. Mulkey, R. M. & Malenka, R. C. (1992) *Neuron* **9,** 967–975.
31. Debanne, D., Gähwiler, B. H. & Thompson, S. M. (1999) *J. Neurosci.* **19,** 10664–10671.
32. Isaac, J. T., Nicoll, R. A. & Malenka, R. C. (1995) *Neuron* **15,** 427–434.
33. Xiao, M.-Y., Wasling, P., Hanse, E. & Gustafsson, B. (2004) *Nat. Neurosci.* **7,** 236–243.
34. Ptashne, M. (1992) *A Genetic Switch: Phage Lambda and Higher Organisms* (Blackwell Scientific, Oxford).
35. Cluzel, P., Surette, M. & Leibler, S. (2000) *Science* **287,** 1652–1655.
36. Ferrell, J. E., Jr., & Machleder, E. M. (1998) *Science* **280,** 895–898.
37. Hodgkin, A. L. & Huxley, A. F. (1952) *J. Physiol.* **117,** 500–544.
38. Koshland, D. E., Jr. (1998) *Science* **280,** 852–853.
39. Bienenstock, E. L., Cooper, L. N. & Munro, P. W. (1982) *J. Neurosci.* **2,** 32–48.
40. Oja, E. (1982) *J. Math. Biol.* **15,** 267–273.
41. Hopfield, J. J. (1982) *Proc. Natl. Acad. Sci. USA* **79,** 2554–2558.